Reachability analysis of an underwater robot with ballast

Luc Jaulin

***Abstract*—When we run a mission with autonomous robots, for security reasons, it is fundamental to guarantee that the state of robot will not enter in a forbidden zone and that it will reach the target area. This problem corresponds to a reachability problem that will be addressed with set-membership uncertainties. In this paper, we show how a serial decomposition can be done to facilitate the resolution. An application related to an underwater robot with a ballast is provided.**

I. Introduction

In this paper, we introduce an efficient method to simulate an underwater robot with interval uncertainties. For simplicity, we consider a situation where the robot has no any sensors, neither exteroceptive nor proprioceptive. The simulation is thus open-loop. The uncertainties, can be either on the initial state vector, on the time-dependent inputs, or on the evolution function.

This problem can be cast into the framework of reachability analysis [6][12][14][4] which is classically used to get a prior prediction of the evolution of a mobile robot. From a mathematical point of view, the problem amounts to integrate a differential inclusion. Compared to other techniques used for the guaranteed integration of differential inclusion [8], the presented approach is simple, fast and accurate. An illustration related to the depth reachability of an underwater robot with a ballast will validate the efficiency of the approach.

II. Ballast robot

We consider an underwater robot equipped with a ballast. The robot can only move upward to the surface and downward to the seafloor. We assume that the state equations [10][7] are given by

$$\begin{cases} \dot{s} &= u \\ \dot{v} &= \frac{s}{1+s} - \frac{1}{1+s} v \cdot \mid v \mid \\ \dot{d} &= v \end{cases} \quad (1)$$

where d is the depth, v is the vertical speed and s is the sinking coefficient (or buoyancy). As illustrated by Figure 1 the buoyancy can be tuned thanks to a piston that can move left or right. The input u corresponds to rate of fluid which enters in the ballast. We assume that we know membership intervals for the initial state variables and a tube (*i.e.*, an interval of trajectories) for the input $u(t)$. Our goal is to find a tube [13][3] for the three state variables.

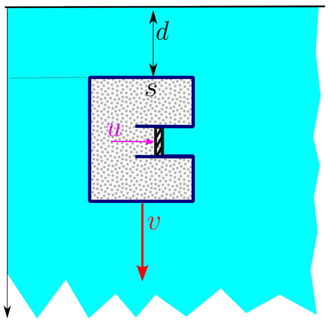

Fig. 1. The buoyancy of the robot may change depending of the position of the piston

III. Differential inclusion

This section recalls some classical results related to differential inclusions [2]. These results will be used further in order to build a reliable procedure to predict the evolution of our robot with interval uncertainties.

We consider the scalar system

$$\begin{aligned} \dot{v}(t) &= f(v(t), \mathbf{u}(t)) \\ v(0) &= v_0 \in [v_0],\ \mathbf{u}(t) \in [\mathbf{u}] \subset \mathbb{R}^m \end{aligned} \quad (2)$$

The signal $\mathbf{u}(t)$ is inside the tube of $\mathbb{R}^m$. Note that $\mathbf{u}(t)$ is chosen as a vector and this is why is it written bold. It varies with time contrary to the box $[\mathbf{u}]$ which is assumed to be constant with time. We have here a differential inclusion [2] with many solutions, as many as we have different signals $\mathbf{u}(t)$ in the box $[\mathbf{u}]$. Finding an envelope for the set of all solutions $v(t)$ is a difficult problem which can be solved using optimal control theory [9] for some cases.

A. Comparison theorem

We recall here a theorem which can be used directly to find an envelope for a differential inclusion with one state variable [5].

Proposition 1. *Assume that the initial condition satisfies* $v_0 \in [v_0^-, v_0^+]$. *An envelope for any solution* $v(t)$ *is given by the interval* $[v^-(t), v^+(t)]$, *where* $v^-(t), v^+(t)$ *satisfy:*

$$\begin{array}{rcl} \dot{v}^- & = & f(v^-, \underset{\mathbf{u}\in[\mathbf{u}]}{argmin} f(v^-, \mathbf{u})) \quad , \quad v(0) = v_0^- \\ \dot{v}^+ & = & f(v^+, \underset{\mathbf{u}\in[\mathbf{u}]}{argmax} f(v^+, \mathbf{u})) \quad , \quad v(0) = v_0^+ \end{array} \tag{3}$$

Proof: The proposition is a consequence of the *Hamilton Jacobi Bellman* theorem in the scalar case [9]. ■

If we define the interval state $\mathbf{z}(t) = [v^-(t), v^+(t)]$, then we have

$$\dot{\mathbf{z}} = \mathbf{g}(\mathbf{z}) \tag{4}$$

where

$$\mathbf{g}(\mathbf{z}) = \begin{pmatrix} f(z_1, \underset{\mathbf{u}\in[\mathbf{u}]}{\text{argmin}} f(z_1, \mathbf{u})) \\ f(z_2, \underset{\mathbf{u}\in[\mathbf{u}]}{\text{argmax}} f(z_2, \mathbf{u})) \end{pmatrix} \tag{5}$$

The function $\mathbf{g}(\mathbf{z})$ will be called the *envelope evolution*.

As a consequence, we can find a good approximation for the two bounds $v^-(t)$ and $v^+(t)$ using any Runge-Kutta method. For instance, we can take the following integration scheme:

$$\mathbf{z}_{t+\delta} \quad = \quad \mathbf{z}_t + \delta \cdot \mathbf{g}\left(\mathbf{z}_t + \frac{\delta \cdot \mathbf{g}(\mathbf{z}_t)}{2}\right) \tag{6}$$

B. Example: the integrator

Consider the integrator

$$\begin{array}{c} \dot{v}(t) = u(t) \\ v(0) = v_0 \in [v_0],\ u(t) \in [u] \subset \mathbb{R} \end{array} \tag{7}$$

Assume that the initial condition satisfies $v_0 \in [v_0^-, v_0^+]$. Any solution $v(t)$ satisfies $v(t) \in [v^-(t), v^+(t)]$, where $v^-(t), v^+(t)$ are defined by

$$\begin{array}{rcl} \dot{v}^- & = & u^- \quad , \quad v(0) = v_0^- \\ \dot{v}^+ & = & u^+ \quad , \quad v(0) = v_0^+ \end{array} \tag{8}$$

The envelope evolution is given by

$$\mathbf{g}(\mathbf{z}) = \mathbf{g}\left(\begin{pmatrix} v^- \\ v^+ \end{pmatrix}, \begin{pmatrix} u^- \\ u^+ \end{pmatrix}\right) = \begin{pmatrix} u^- \\ u^+ \end{pmatrix}$$

C. Example: the sinking body

We consider a body totally immersed in the ocean as represented by Figure 2. As it will be seen later this example is chosen since it is an important component of our underwater robot.

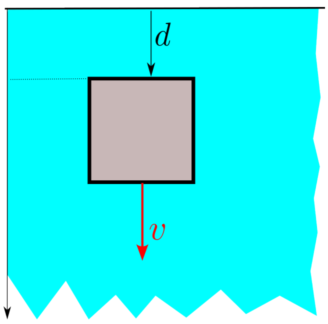

Fig. 2. Sinking body

The speed v of the body satisfies the following differential equation

$$\dot{v} = a - bv|v| \tag{9}$$

where $b > 0$ corresponds to a dumping coefficient. If the body has a negative buoyancy, the coefficient a is positive and the body sinks toward the bottom. If it has a positive buoyancy, a is negative and the body goes up toward the surface. We assume that both are known to belong to the intervals $[a^-, a^+]$, and $[b^-, b^+]$, respectively.

Taking into account Proposition 1, we get that the trajectory $v(t)$ is bounded by the two functions v^- and v^+ defined by

$$\begin{array}{rclcl} \dot{v}^- & = & \underbrace{a^- - b^+ \cdot v^- |v^-|}_{f^-_{[a],[b]}(v^-)} & , & v^-(0) = v_0^- \\ \dot{v}^+ & = & \underbrace{a^+ - b^- v^+ |v^+|}_{f^+_{[a],[b]}(v^+)} & , & v^+(0) = v_0^+ \end{array} \quad (10)$$

The envelope evolution is given by

$$\begin{array}{rcl} \mathbf{g}(\mathbf{z}) & = & \mathbf{g}\left(\left(\begin{array}{c} v^- \\ v^+ \end{array}\right), \left(\begin{array}{c} a^- \\ a^+ \\ b^- \\ b^+ \end{array}\right)\right) \\ & = & \left(\begin{array}{c} a^- - b^+ \cdot v^- |v^-| \\ a^+ - b^- v^+ |v^+| \end{array}\right) \end{array}$$

We consider four cases.

Case a. We have $(v_0, a, b) \in [0.9, 1.1] \times [0.9, 1.1] \times [1.9, 2.1]$. This means that for $t = 0$, the body goes to the bottom. Since $a > 0$, it sinks (as represented by stones in the cube). The two trajectories $v^-(t)$,$v^+(t)$ in red are obtained by the Runge-Kutta integration (6). We observe that the velocity interval $[v^-(t), v^+(t)]$ converges to the interval $[\bar{v}] = \text{sign}([a])\sqrt{\frac{|[a]|}{[b]}}$.

Case b. We have $(v_0, a, b) \in [-1.1, -0.9] \times [-1.1, -0.9] \times [1.9, 2.1]$. This means that for $t = 0$, the body goes to the surface. Since $a < 0$, it floats (as represented by the bubbles in the cube). Again, the two trajectories $v^-(t)$,$v^+(t)$ in red are obtained by the Runge-Kutta integration (6). And again, we observe that $v(t)$ converges to a value $\bar{v}$.

Case c. We have $(v_0, a, b) \in [0.9, 1.1] \times [-1.1, -0.9] \times [1.9, 2.1]$. For $t = 0$, the body is thrown toward the bottom. Since $a < 0$, the body floats. We observe that after approximately 1 sec, the body stops sinking and then starts its course to the surface. For the simulation, we need to compute the time at which $v(t)$ changes its sign.

Case d. We have $(v_0, a, b) \in [-1.1, -0.9] \times [0.9, 1.1] \times [1.9, 2.1]$. For $t = 0$, the body is thrown toward the surface. Since $a > 0$, the body sinks. We observe that after approximately 1 sec, the body stops surfacing and then starts its course to the bottom.

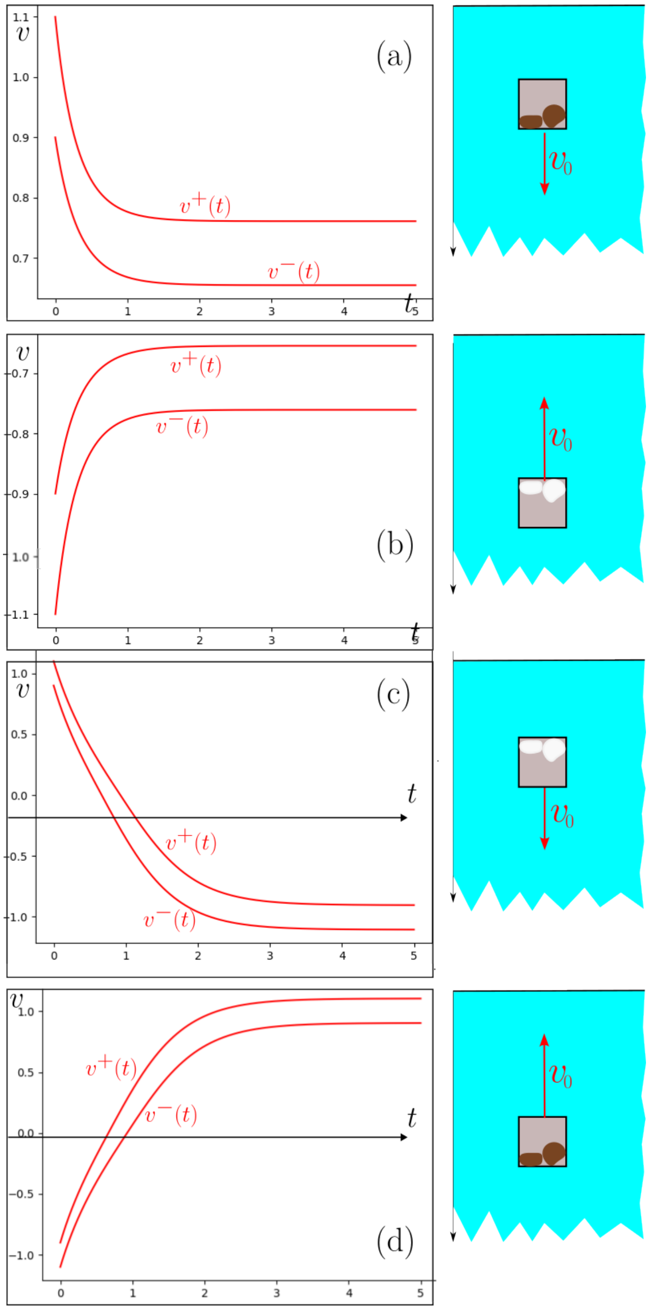

Fig. 3. Sinking body (with stones inside) or floating body (with bubbles inside) for different initializations. The tubes contains the trajectory $v(t)$

IV. Interval simulation of the ballast robot

We will take advantage of the fact that our system is composed of three SISO (Single-Input Single-

Output) systems in series, as illustrated by Figure 4. We have

$$\begin{array}{rcl} \dot{s}^- & = & u^- \\ \dot{s}^+ & = & u^+ \\ \dot{v}^- & = & \mathrm{lb}\left(\frac{[s]}{1+[s]} - \frac{1}{1+[s]} \cdot v^- \cdot \mid v^- \mid\right) \\ \dot{v}^+ & = & \mathrm{ub}\left(\frac{[s]}{1+[s]} - \frac{1}{1+[s]} \cdot v^+ \cdot v^+ \mid\right) \\ \dot{d}^- & = & v^- \\ \dot{d}^+ & = & v^+ \end{array}$$

where *lb* and *ub* are the lower bound and the upper bound of the corresponding intervals. In this formulation, we have used interval operations [11] inside the expression of the envelope evolution. We can rewrite the system, without using interval arithmetic, as follows:

$$\underbrace{\begin{pmatrix} \dot{s}^- \\ \dot{s}^+ \\ \dot{v}^- \\ \dot{v}^+ \\ \dot{d}^- \\ \dot{d}^+ \end{pmatrix}}_{\dot{\mathbf{z}}} = \underbrace{\begin{pmatrix} u^- \\ u^+ \\ \frac{s^-}{1+s^-} - \max\begin{pmatrix} \frac{v^-\cdot|v^-|}{1+s^-} \\ \frac{v^-\cdot|v^-|}{1+s^+} \end{pmatrix} \\ \frac{s^+}{1+s^+} - \min\begin{pmatrix} \frac{v^+\cdot|v^+|}{1+s^-} \\ \frac{v^+\cdot|v^+|}{1+s^+} \end{pmatrix} \\ v^- \\ v^+ \end{pmatrix}}_{\mathbf{g}(\mathbf{z})}$$

This expression can be obtained easily in our particular case, where the monotonicity analysis is simple. In the general case, interval arithmetic is needed to get the envelope evolution. An integration can now be obtained using a Runge-Kutta method.

The behavior of the interval simulator is illustrated by Figure 4. We took $[s_0] = [v_0] = [d_0] = [0, 0.1]$ for the initial conditions. For the input, we took $[u](t) = \sin(t)+[-0.1, 0.1]$. Even if the system is unstable, we do not observe any exponential explosion of the pessimism, contrary to other existing interval methods dealing with differential inclusions.

V. Conclusion

In this paper, we have proposed a new approach to compute an envelop for the set of all feasible trajectories to a robot under interval uncertainties. If we define the *reach set* $\mathbb{X}(t)$ as the set of all state vectors $\mathbf{x}(t)$ that can be reached at time t, then, we are able to compute a box $[\mathbf{x}](t)$ which encloses $\mathbb{X}(t)$, *i.e.*,

$$\mathbb{X}(t) \subset [\mathbf{x}](t) = [x_1^-(t), x_1^+(t)] \times \cdots \times [x_n^-(t), x_n^+(t)].$$

The method is based on an extended state $\mathbf{z}(t) = \left(x_1^-(t), x_1^+(t), \ldots, x_n^-(t), x_n^+(t)\right)$ of dimension $2n$. This extended state satisfies an ordinary differential equation of the form $\dot{\mathbf{z}} = \mathbf{g}(\mathbf{z})$ which we can easily be integrated using an integration method such as a Runge-Kutta method.

Note that the Runge-Kutta method can be considered as reliable in practice, but the approach cannot guarantee that no feasible trajectory has been lost. To be completely rigorous, we have to use a guaranteed interval integration method such as that proposed in [8] or [1] for the integration of $\mathbf{z}$.

The Python source codes of the example are available at

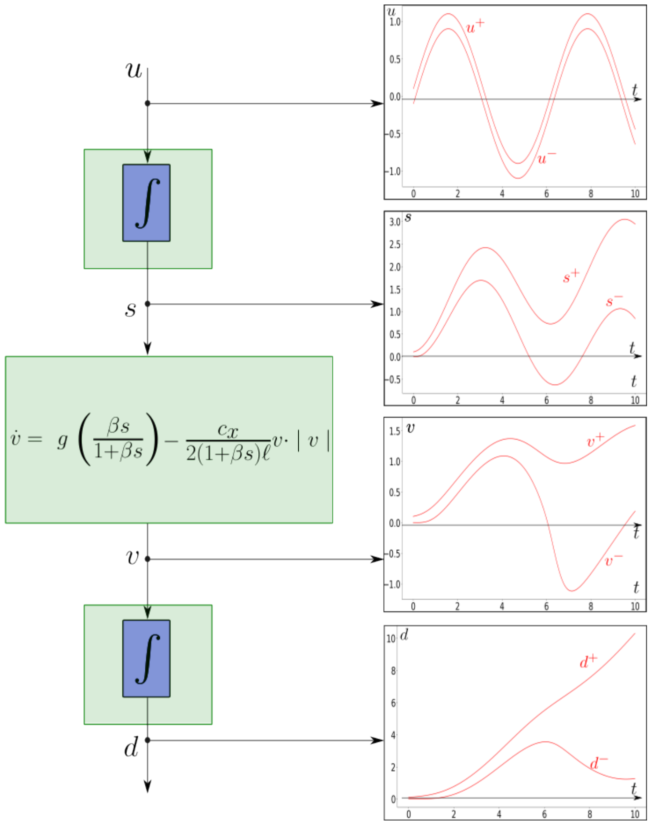

Fig. 4. The robot is composed of three SISO systems in series; The tubes contain the trajectories $u(t), s(t), v(t), d(t)$

https://www.ensta-bretagne.fr/jaulin/ocean25.html

REFERENCES

[1] J. Alexandre dit Sandretto and A. Chapoutot. Dynibex: a differential constraint library for studying dynamical systems. In *Conference on Hybrid Systems: Computation and Control*, Vienne, Austria, 2016. V

[2] J.P. Aubin and H. Frankowska. *Set-Valued Analysis*. Birkhäuser, Boston, Boston, MA, 1990. III, III

[3] Fabrice Le Bars. *Analyse par intervalles pour la localisation et la cartographie simultanées ; Application à la robotique sous-marine*. PhD dissertation, Université de Bretagne Occidentale, Brest, France, 2011. II

[4] J. Damers, L. Jaulin, and S. Rohou. Lie symmetries applied to interval integration. *Automatica*, 144, 2021. I

[5] D. Efimov and T. Raïssi. Design of interval observers for uncertain dynamical systems. *Automation and Remote Control*, 77(2):191–225, 2016. III-A

[6] G. Frehse. Phaver: Algorithmic verification of hybrid systems. *International Journal on Software Tools for Technology Transfer*, 10(3):23–48, 2008. I

[7] L. Jaulin. *RobMOOC, un MOOC sur la commande non-linéaire des robots mobiles* , www.ensta-bretagne.fr/robmooc/. ENSTA-Bretagne, 2019. II

[8] T. Kapela, M. Mrozek, D. Wilczak, and P. Zgliczynski. CAPD: dynsys, A flexible C++ toolbox for rigorous numerical analysis of dynamical systems. *Communications in Nonlinear Science and Numerical Simulation*, 101:105578, 2021. I, V

[9] S. LaValle. *Planning Algorithm*. Cambridge University Press, 2006. III, III-A

[10] T. Le Mézo, G. Le Maillot, T. Ropert, L. Jaulin, A. Ponte, and B. Zerr. Design and control of a low-cost autonomous profiling float. *Mechanics and Industry*, 21(5), 2020. II

[11] R. Moore. *Methods and Applications of Interval Analysis*. Society for Industrial and Applied Mathematics, jan 1979. IV

[12] A. Rauh, J. Kersten, and H. Aschemann. Techniques for verified reachability analysis of quasi-linear continuous-time systems. In *2019 24th International Conference on Methods and Models in Automation and Robotics*, pages 18–23, 2019. I

[13] S. Rohou, L. Jaulin, L. Mihaylova, F. Le Bars, and S. Veres. *Reliable Robot Localization*. Wiley, dec 2019. II

[14] W. Taha and A. Duracz. Acumen: An open-source testbed for cyber-physical systems research. In *Conference on CYber physiCaL systems, iOt and sensors Networks*, 2015. I